Effect of Temperature on AuPd Nanoparticles Produced by Inert Gas Condensation

Eduardo Pérez-Tijerina,*,† Sergio Mejía-Rosales,*,‡,† Hiromi Inada,§,|| and Miguel José-Yacamán‡

Center for Innovation and Research in Engineering and Technology and Facultad de Ciencias Físico-Matemáticas, Universidad Autónoma de Nuevo León, San Nicolás de los Garza, N. L., México 66450, Department of Physics and Astronomy, University of Texas at San Antonio, San Antonio, TX 78249, Hitachi High Technologies America, Inc., Pleasanton, CA 94588, and Center for Functional Nanomaterials, Brookhaven National Laboratory, Upton, NY 11973

Received: February 2, 2010; Revised Manuscript Received: March 9, 2010

Bimetallic nanoparticles of AuPd were synthesized using the inert gas condensation technique, where the material is sputtered from a target and the particles are formed in an inert condensation zone. Throughout the synthesis process and jointly with the control of the atmosphere conditions, the region after the condensation chamber was kept at a fixed temperature, and several experimental runs were performed at 700 and 1000 °C. The synthesis conditions were set to produce particles of 5 nm of diameter, and almost all of the resulting nanoparticles were icosahedral in shape with small deviations from the mean size. We analyzed the particles by high-angle annular dark field and bright field scanning electron microscopy imaging with a resolution high enough to acquire atomic detail and to measure the distance between planes. From the micrographs and their fast Fourier transform patterns, we found that the lattice detail depends on the thermal treatment with larger lattice fringe displacements in the particles produced at 700 °C. Electron energy loss spectroscopy analysis in one and two dimensions shows that irrespective of the temperature the particles keep their icosahedral shape, and both chemical species are distributed nonuniformly all over the volume of the particles, but without forming core−shell structures.

Introduction

It is a well-established fact that the structural detail of metal nanoparticles depends not only on the thermal conditions, but also on the kinetic processes involved in the method of synthesis.[1,2] This is particularly relevant in the case of bimetallic nanoparticles, where the local concentration of the atomic species may vary from core−shell structures to almost uniform distributions, with a large set of intermediate possibilities that includes well-defined multiple shells, concentration gradients, or even particles with voids.[3] Distribution of the chemical elements is not the only issue that is influenced by the kinetics, but also the shape of the particles and the structure of the surface, and hence the most of the chemical properties of the nanoparticles. Thus, in order to adequately exploit the features of a particular synthesis technique to produce particles for specific purposes, an in-depth characterization is needed.

Several techniques based on wet chemistry allow the production of bimetallic Au/Pd nanoparticles with a relatively good control on the size and with a local core−shell distribution, despite the negative value of the bulk mixing energy that makes the alloying of the two metals a more energetically favorable distribution.[4] Besides this, in the particles produced by these techniques the final proportions of the chemical species can only be investigated a posteriori. On the other hand, physical methods of synthesis such as inert gas condensation (IGC) allow even narrower size distributions than those obtained by chemical methods, and the elemental proportions follow those of the original alloy used as target. Previous results from our group[5] show that for the case of Au/Pd particles produced by IGC at room temperature both metals are distributed throughout the entire particle with a fairly homogeneous distribution; nevertheless, at the time there was not enough information to estimate the concentration profiles at high resolution.

Several processes in the interior of the IGC chamber are involved in the condensation of the particles, such as coagulation of small clusters, and impacts with the Ar and H molecules that conform the controlled atmosphere. The ratio of these processes, and the thermal energy available to rearrange the metal atoms during the condensation, will have a determining effect on the final shape and the inner structure of the particles. Molecular dynamics (MD) simulations of the heating of Au/Pd particles show that if the temperature is high enough the gold atoms may be able to migrate to the outer shells of the particles and the palladium atoms will tend to be concentrated at the core.[6] Recent simulations based on interatomic potentials fitted both experimentally and by DFT calculations predict segregation of Au to the surface without necessarily forming a core−shell structure.[7] On the other hand, MD simulations of impacts between Au and Pd clusters predict that the resulting particles will be made of a uniform alloy.[4] Thus, it is likely that the interplay between minimization of surface energy, mixing entalphy, and kinetic effects will determine the final shape of the particles, their size, and the spatial distribution of the atomic species.

In this paper, we report the production by IGC of Au/Pd nanoparticles structured as alloys with both metals present at the whole of each particle. For the synthesis of the particles, we performed two sets of experimental runs, one keeping the

* To whom correspondence should be addressed: E-mail: (E.P.-T.) eduardo.pereztj@uanl.edu.mx; (S.M.-R.) sergio.mejiarosales@utsa.edu.
† Universidad Autónoma de Nuevo León.
‡ University of Texas at San Antonio.
§ Hitachi High Technologies America, Inc.
|| Brookhaven National Laboratory.

10.1021/jp101003g © 2010 American Chemical Society
Published on Web 03/31/2010

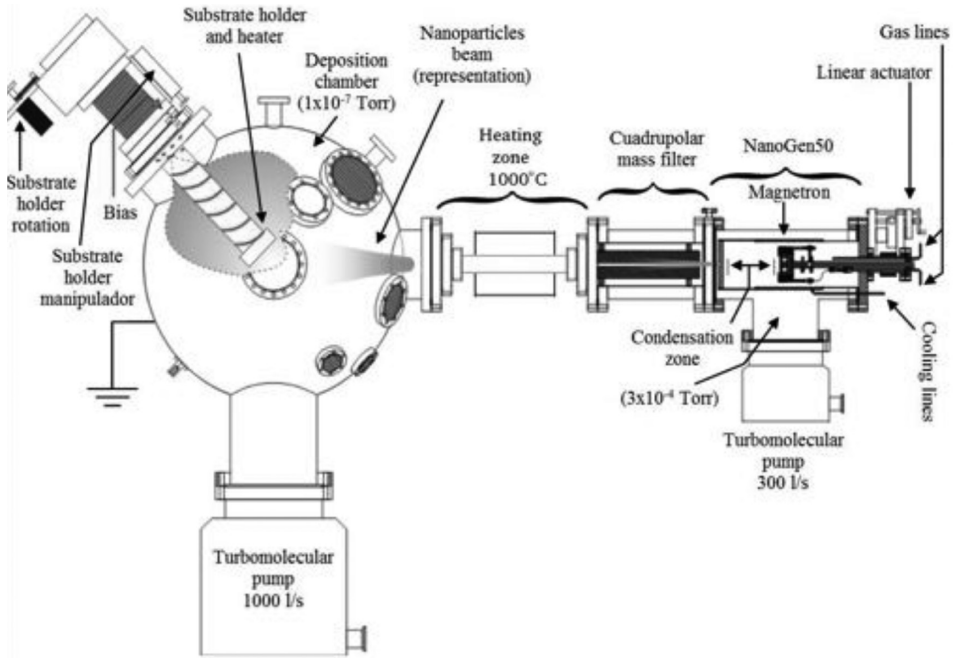

Figure 1. Diagram of the experimental setup for the ICG production and in-flight heating of nanoparticles.

region immediately after the condensation chamber at 700 °C, and the other at a temperature of 1000 °C. In the following sections, we will detail the experimental setup and methods, and the analysis performed to investigate the shape, structure, and composition of the particles.

Experimental Setup

The condensation of the nanoparticles was performed in a Nanogen500 system, manufactured by Mantis Deposition LTD.[8] In this system, the metal atoms are sputtered from the alloy target and directed into the condensation chamber, which is kept at a controlled atmosphere of argon and helium. The particles produced at the condensation chamber are selected by mass by a quadrupolar filter, and a differential pressure makes the particles reach the deposition chamber. Details of the sputtering and condensation processes can be found elsewhere.[8–11]

After the production in the synthesis chamber and after the particles were filtered by mass, the particles were heated while in-flight at a controlled temperature. The length of heating zone is 30 cm approximately and since the velocity of the particles lay on the range of 100−500 m/s, the heating time was of a few milliseconds. The diagram of this experimental setup is shown in Figure 1. An alloy target of $Au_{50\%}$—$Pd_{50\%}$, manufactured by Aci Alloys with a 99.99% purity, was used for all the experimental runs. The time of deposition was adjusted to produce a low rate of deposition of particles to lower the probability of interaction between particles at the moment of the deposition and to avoid coalescence while the samples are observed by electron microscopy. Standard holey carbon microgrids 200 mesh produced by EMS, made by a fine layer of amorphous carbon deposited onto a copper substrate with numerous holes of different sizes, were used as substrates. Figure 2 shows a low-magnification micrograph of a typical region of one of the samples that confirms that the deposition was indeed made at a low rate.

Depositions were made at 700 and 1000 °C, and the synthesis parameters, voltage, partial pressure, and active region length, were fine-tuned to produce particles of 5 nm of diameter. The particles were deposited directly in the carbon grids to be analyzed later by annular dark field (ADF) and bright field (BF) scanning transmission electron microscopy (STEM) microscopy. The images were obtained with an aberration-corrected Hitachi HD-2700C STEM system.[12] Simultaneously with the acquisition of the ADF and BF STEM images, one- and two-dimensional electron energy loss spectroscopy (EELS) analysis was performed on several particles selected by their orientation. Figure 3 shows high-resolution ADF and bright-field STEM images of some of the particles, where it can be easily noted that the resolution is indeed high enough to resolve the atomic planes.

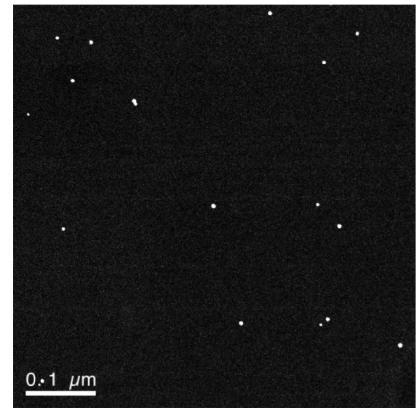

Figure 2. Low-magnification ADF-STEM micrograph of a typical region of the sample. Bright spots correspond to Au−Pd nanoparticles.

Results

Annealing at 700 °C. Figure 4 shows high-magnification images and the corresponding Fourier transforms of three of the particles heated at 700 °C in flight before deposition. As can be noted, the structure of the particles is very well-defined, and both the real space and the reciprocal space images have the enough resolution to allow to measure the lattice parameters at subangstrom detail. The measured lattice constants were 2.33 and 1.44 nm, as remarked in Figure 4. These distances correspond to the {111} and {220} planes of Au, respectively.

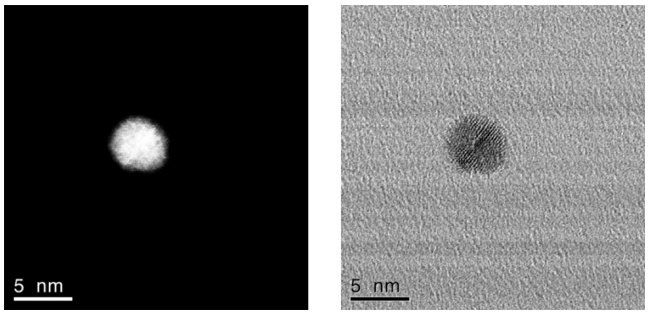

Figure 3. ADF and BF STEM images of a typical Au−Pd particle produced by inert gas condensation.

From the intensity profile of the ADF-STEM image, it can be noted that the particles are unlikely to have a core−shell structure, unlike Au−Pd particles of similar size produced by different methods.[13] It is also interesting to note the presence of isolated atoms in the immediate vicinity of the particles, highlighted in Figure 4 with white circles. The distribution of the chemical elements was investigated by EELS, and one result for the EELS line profile of Pd is shown in Figure 5. For purposes of comparison, the figure also shows the high-angle annular dark field (HAADF) intensity line profile of the same particle. From the EELS profile it can be noted that, although Pd seems to be distributed throughout the entire particle, this distribution appear to be nonuniform, since the Pd map indicates separation around the 2 nm mark, close to the center of the particle. EELS one-dimensional profiles of Au were also carried out, but the Au signal is very weak compared to that of Pd. Nevertheless, the EELS detector was able to measure a Au-M4,5 core loss signal strong enough to allow to make an interpretation of the line profile. While the Au profile indicated the presence of Au in the entire volume of the particle, the signal-to-noise ratio was relatively low, and so a high-resolution profile was not possible; however, from the comparison between the Pd EELS profile and the HAADF profile, it can be inferred that there exists a region close to the center of the particle rich in gold but with some degree of mixing with Pd.

Annealing at 1000 °C. When the in-flight annealing temperature was set to 1000 °C, the particles kept their quasi-icosahedral shape, as can be seen in Figure 6. In these high-magnification HAADF-STEM micrographs, the orientation of the particles, different from that of the particles shown in Figure 4, allows one to discern the atomic columns forming the (111) layers of the quasi-icosahedral particles, and the resolution is high enough to reveal that the surface is somewhat rough. The intensity of the STEM images of the particles shows that in these particles both chemical species are distributed throughout the entire volume of the particles (there are not definite regions

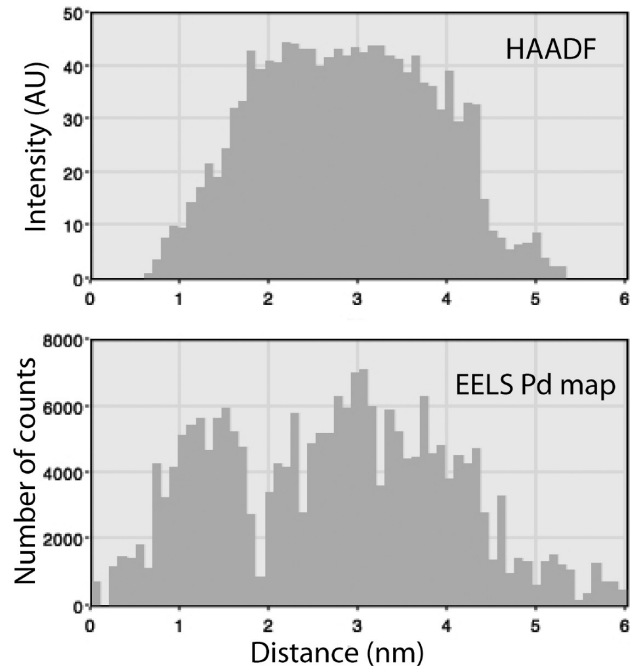

Figure 5. Linear Pd EELS profile (335 eV) performed on one of the particles annealed at 700 °C, and its corresponding HAADF intensity profile.

of high intensity related to the predominance of Au) as in the particles heated at 700 °C, but unlike the latter the particles annealed at 1000 °C appear to have lattice constants of 2.20 and 1.40 nm, as can be noted in the inset of Figure 6. The EELS mapping of the particles annealed at 1000 °C shows that both gold and palladium are indeed present all over the particles, and while there is a nonuniform distribution of the chemical species, there is not a definite spatial separation of the elements. Figure 7 shows one of the EELS maps obtained for the Pd-M4,5 characteristic energy (335 eV). Again, the EELS gold signal at 2206 eV turns out to be weak, as expected for a heavy element, but high enough to show the presence of Au at any place inside the particle.

Discussion and Conclusions

Unlike the chemical methods for the production of binary nanoalloys, where the order in which the metals are incorporated strongly determine the formation of core−shell structures, in an inert gas condensation synthesis process there is not a pre-established order in the addition of the chemical elements, and so the elemental distribution in the volume of the particles will be mostly determined by the kinetic processes taking place on the interior of the condensation chamber with both metals

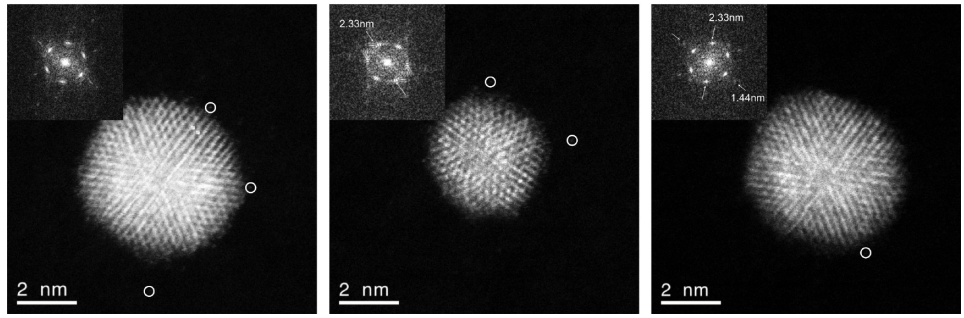

Figure 4. High-resolution ADF-STEM micrographs of three of the particles annealed at 700 C and their corresponding FFT. The white circles in the micrograph remark the presence of isolated atoms in the vicinity of the surface of the particle.

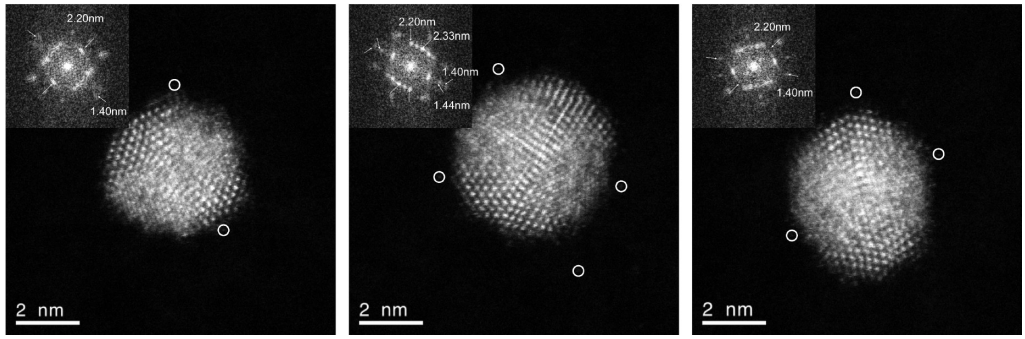

Figure 6. High-resolution ADF-STEM micrographs of three of the particles annealed at 1000 C, and their corresponding FFT. The white circles in the micrograph remark the presence of isolated atoms in the vicinity of the surface of the particle.

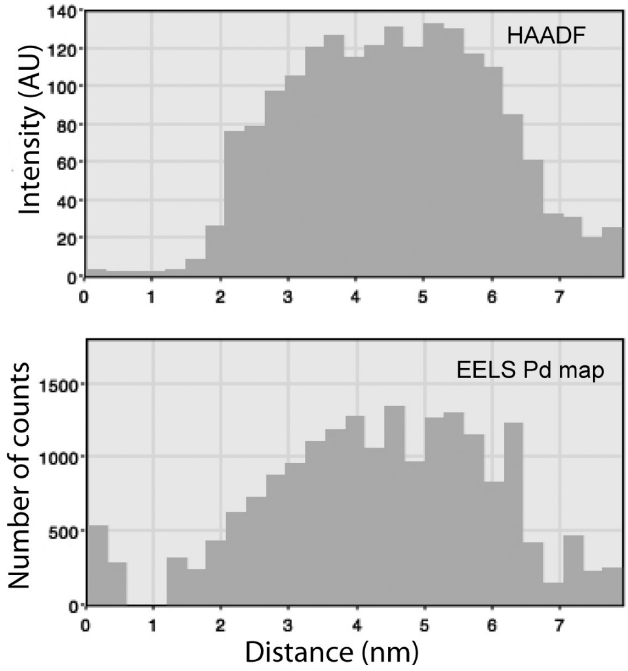

Figure 7. Linear Pd EELS profile (335 eV) performed on one of the particles annealed at 700 °C, and its corresponding HAADF intensity profile.

present at a time. In a previous work, we showed that for the particular case of Au/Pd nanoalloys prepared by IGC at room temperature, the resulting particles presented a highly homogeneous distribution of both metals on the whole of the volume of the particles.[5] In this work, we have found that the in-flight annealing of the particles supply the kinetic energy needed for the metals to redistribute to certain degree, but without forming a core−shell distribution. We found that the temperature of in-flight annealing of the particles does not have a determining effect on the specific details of the distribution of gold and palladium, at least at the temperatures used in this study, but the lattice fringe distances (lattice constants) may indeed depend on the annealing temperature. For the particles heated at 700 °C, the lattice fringe displacements, measured on the fast Fourier transform (FFT) of the STEM micrographs, gave distances of 2.33 and 1.44 nm; for the particles treated at 1000 °C, the distances are 2.20 and 1.40 nm. In some of the particles, both sets of distances are present, which is likely to be due to the coexistence of two structural phases.

Another relevant result of this work is related to the final shape of the annealed particles. Even when a transformation from icosahedra to decahedra when the temperature is risen to values just below the melting point has been reported in gold[14,15] and nickel particles,[16] and attempts have been made to construct phase maps with definite icosahedral and decahedral regions,[17] there is no actual consensus about how the appearance of icosahedra depends on the thermal conditions or the size of the particles. In this work, we have found that even after the annealing of the particles at the sizes and composition considered in this work, the nanoparticles still keep their icosahedral shape. This situation is likely to change in larger particles, where the stresses to which the inner atoms are subjected become too large, and the energy due to these stresses make it impossible to maintain the low surface energy (111) facets of an icosahedron.[18]

The fact that both gold and palladium remain distributed in the totality of the volume of the particles produced by ICG after the thermal treatment is particularly relevant when the catalytic properties of the nanoalloy are considered. It is known that the catalytic activity of Pd is affected by the presence of Au atoms,[19] and that the presence of Pd at the surface of the particles gets favored when the Pd atoms can bond with gold atoms.[20] The availability of an experimental method that promotes the production of particles where both chemical elements are present at the surface and simultaneously keeps a high control in the mean size and geometry of the particles may allow a more efficient use of the alloys as catalysts for specific reactions.

Acknowledgment. This work was supported by the International Center for Nanotechnology and Advanced Materials (ICNAM) of the University of Texas at San Antonio, the Welch Foundation (Grant AX-1615), the Mexican Council for Science and Technology (CONACYT, exp. 119100), and the Council for Science and Technology of the State of Nuevo León, México.

References and Notes

(1) Ferrando, R.; Jellinek, J.; Johnston, R. L. Nanoalloys: From Theory to Applications of Alloy Clusters and Nanoparticles. *Chem. Rev.* **2008**, *108*, 845–910.

(2) Burda, C.; Chen, X.; Narayanan, R.; El-Sayed, M. A. Chemistry and Properties of Nanocrystals of Different Shapes. *Chem. Rev.* **2005**, *105*, 1025–1102.

(3) José-Yacamán, M.; Pérez-Tijerina, E.; Mejía-Rosales, S. Defect structure in nanoalloys. *J. Mat. Chem.* **2007**, *17*, 1035–1038.

(4) Mariscal, M. M.; Oldani, N. A.; Dassie, S. A.; Leiva, E. P. M. Atomistic computer simulations on the generation of bimetallic nanoparticles. *Faraday Discuss.* **2008**, *138*, 89–104.

(5) Pérez-Tijerina, E.; Gracia Pinilla, M.; Mejía-Rosales, S.; Ortiz-Méndez, U.; Torres, A.; José-Yacamán, M. Highly size-controlled synthesis of Au/Pd nanoparticles by inert-gas condensation. *Faraday Discuss.* **2008**, *138*, 353–362.

(6) Mejía-Rosales, S. J.; Fernández-Navarro, C.; Pérez-Tijerina, E.; Montejano-Carrizales, J. M.; José-Yacamán, M. *J. Phys. Chem. B* **2006**, *110* (26), 12884–9.

(7) Pittaway, F.; Paz-Borbón, L. O.; Johnston, R. L.; Arslan, H.; Ferrando, R.; Mottet, C.; Barcaro, G.; Fortunelli, A. *J. Phys. Chem. C* **2009**, *113*, 9141–9152.

(8) Mantis Deposition Ltd. Oxford, England. www.mantisdeposition.com (accessed November 1, 2009).
(9) Shyjumon, I. Ph.D. Thesis, University of Greifswald, Greifswald, Germany, 2005.
(10) Barker, S. H.; Thorton, S. C.; Keen, A. M.; Preston, T. I.; Norris, C.; Edmonds, K. W.; Binns, C. *Rev. Sci. Instrum.* **1997**, *68*, 1853–1857.
(11) Goldby, I. M.; Von Issendorff, B.; Kuipers, L.; Palmer, R. E. *Rev. Sci. Instrum.* **1997**, *68*, 3327–3334.
(12) Inada, H.; Wu, L.; Wall, J.; Su, D.; Zhu, Y. *J. Electron Microsc.* **2009**, *58*, 111–122.
(13) Ferrer, D.; Blom, D. A.; Allard, L. F.; Mejía, S.; Pérez-Tijerina, E.; José-Yacamán, M. *J. Mater. Chem.* **2008**, *18*, 2442–2246.
(14) Koga, K.; Ikeshoji, T.; Sugawara, K. *Phys. Rev. Lett.* **2004**, *92*, 115507.
(15) Inasawa, S.; Sugiyama, M.; Yamaguchi, Y. *J. Phys. Chem. B* **2005**, *109*, 3104–3111.
(16) Schebarchov, D.; Hendy, S. C. *Phys. Rev. Lett.* **2005**, *95*, 116101.
(17) Barnard, A. S.; Young, N. P.; Kirkland, A. I.; van Huis, M. A.; Xu, H. *ACS Nano* **2009**, *3*, 1431–1436.
(18) Henry, C. Size Effects on Structure and Morphology of Free or Supported Nanoparticles. In *Nanomaterials and Nanochemistry*; Bréchignac, C., Houdi, P., Lahmani, M., Eds.; Springer: Berlin/Heidelberg, 2008.
(19) Enache, D. I.; Edwards, J. K.; Landon, P.; Solsona-Espriu, B.; Carley, A. F.; Herzing, A. A.; Watanabe, M.; Kiely, C. J.; Knight, D. W.; Hutchings, G. J. *Science* **2006**, *311*, 362.
(20) Yuan, D.; Gong, X.; Wu, R. *Phys. Rev. B* **2008**, *78*, 035441.

JP101003G